

New mononuclear Pd(II) and Pt(II) complexes with a N-heterocyclic thiosemicarbazone: cytotoxicity, solution behaviour and interaction versus proven models from the biological media

Ana I. Matesanz^a; Eva Jimenez-Faraco^a; María C. Ruiz^b; Lucia M. Balsa^b Carmen Navarro-Ranninger^a; Ignacio E. León^{b*}; A.G. Quiroga^{a*}

SUPPLEMENTARY MATERIAL

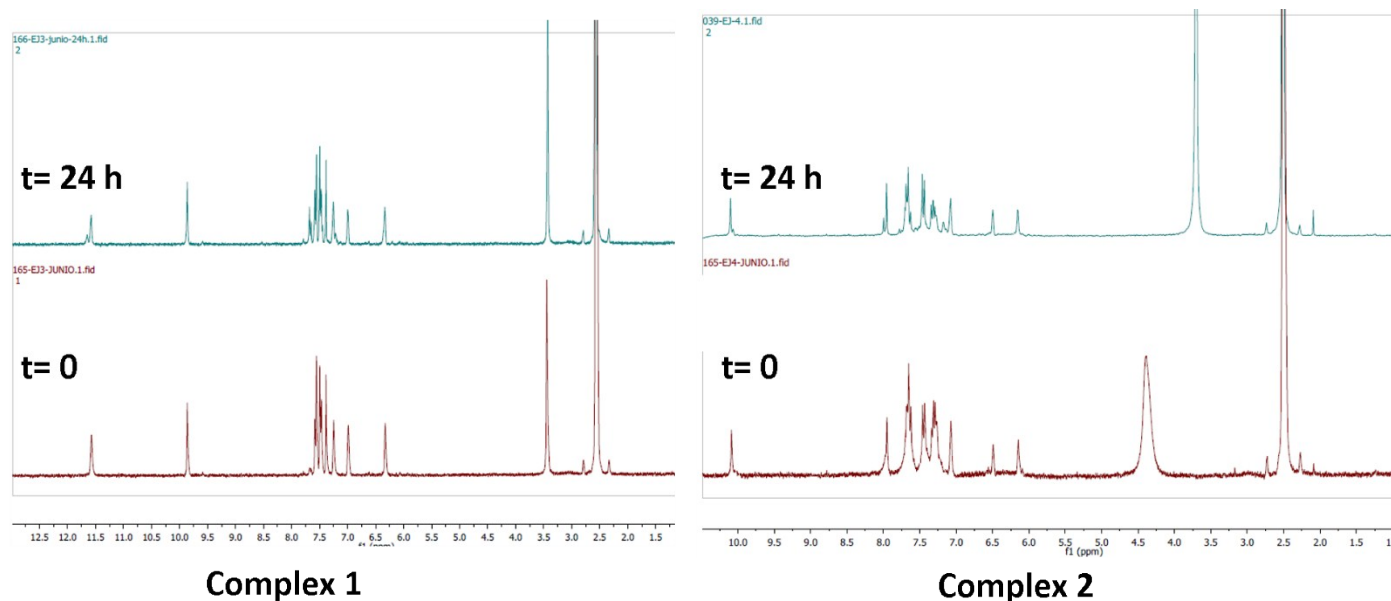


Figure SM1. ¹H NMR spectra of complexes **1** and **2** at t=0 and 24h in DMSO-d₆.

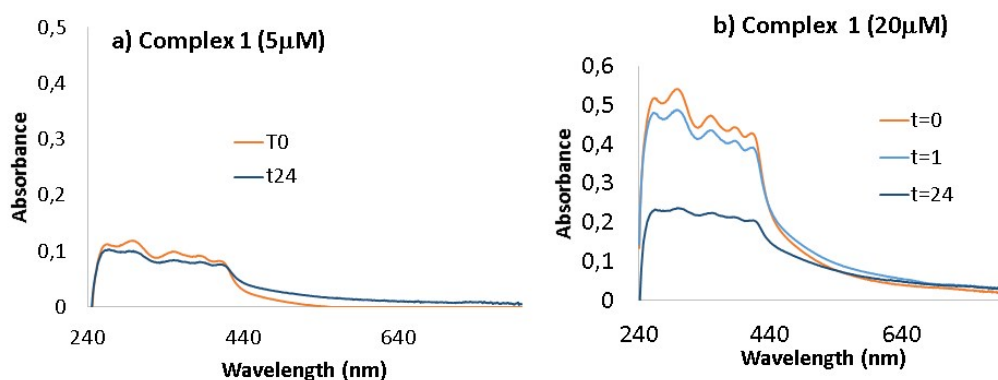


Figure SM2. UV/Vis spectra analysis from fresh to 24h of complex **1** in Tris buffer solution at a) 5 μM and b) 20 μM

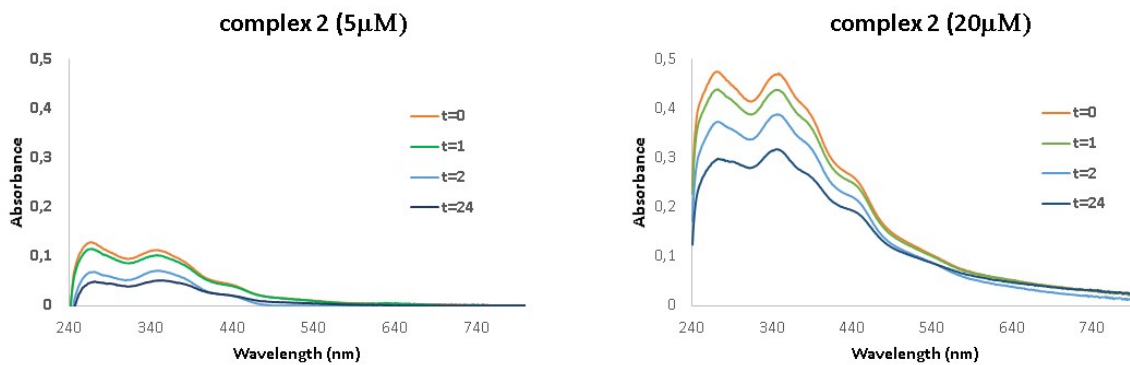


Figure SM3. UV/Vis spectra analysis from fresh to 24h of complex **2** in Tris buffer solution at a) 5 μ M and b) 20 μ M.

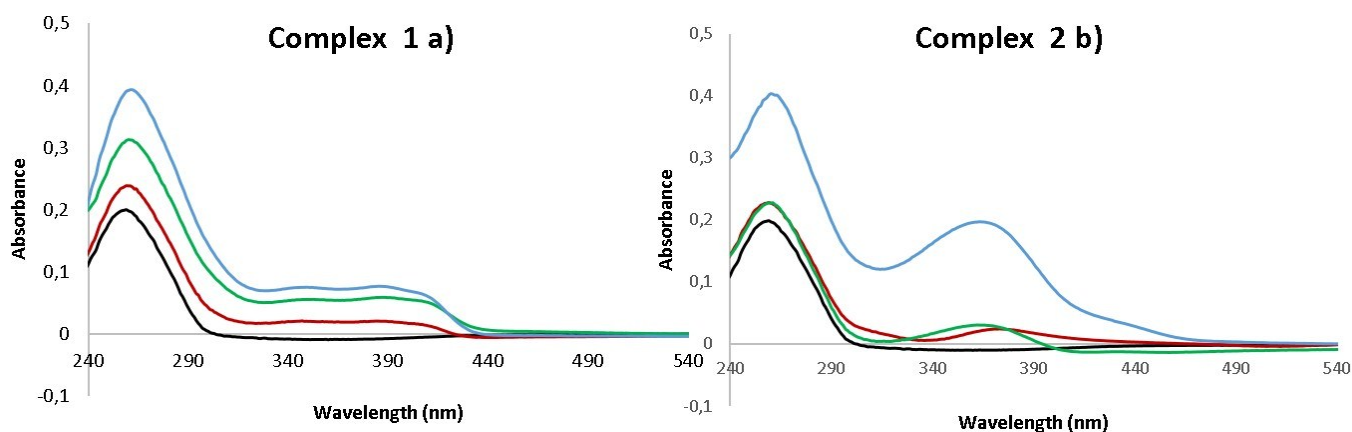


Figure SM4. UV/Vis absorption spectra of CT-DNA in the absence (bottom line) and presence of the (a) complex **1** and (b) complex **2**, using of increasing amounts of r values: [complex]/[CT-DNA] (from bottom to top): 0.5, 0.2 and 0.14.

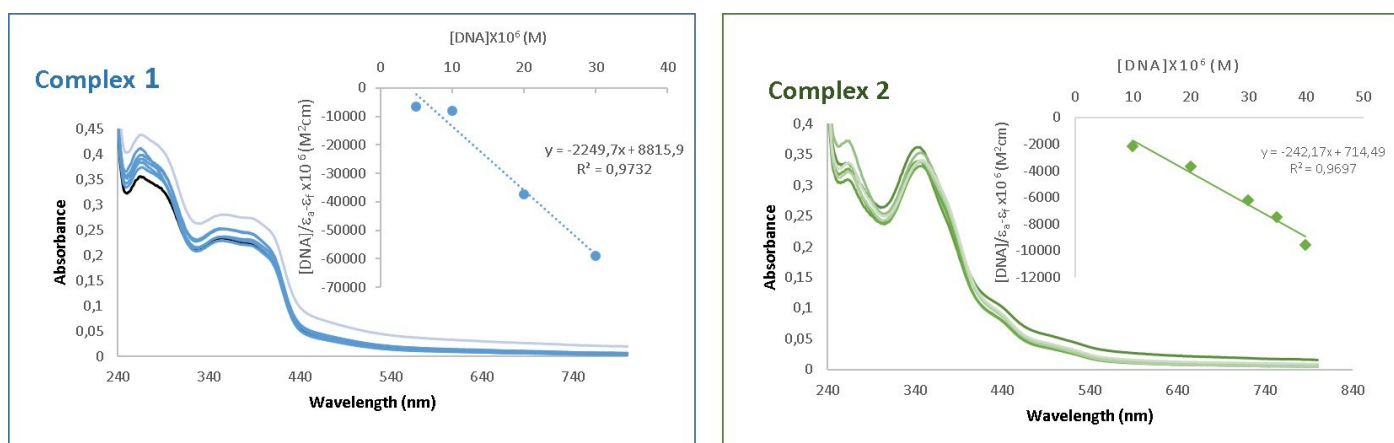


Figure SM5. UV/Vis absorption spectra of complex **1** and **2** in the presence of increasing amounts of compound CT-DNA. The data were collected for [complex] = 2.5×10^{-6} M and [CT-DNA] = 10-40 μ M. The insert shows a fitting of the absorbance data used to obtain the binding constant.

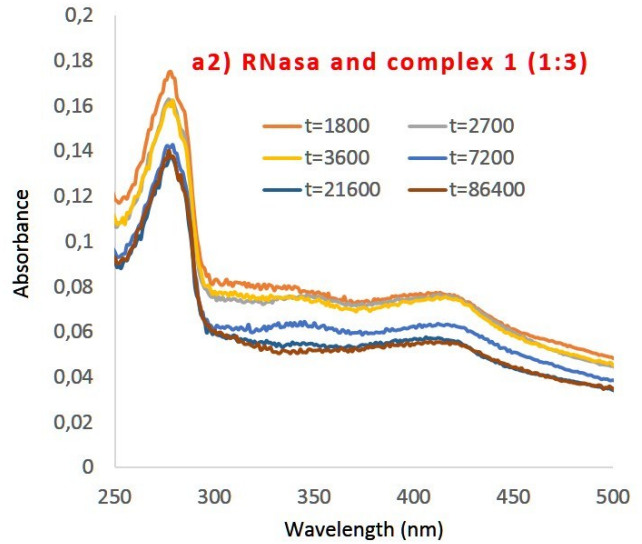
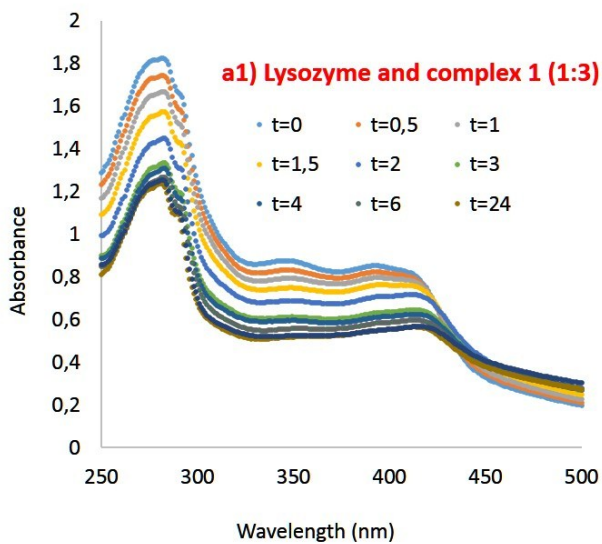


Figure SM6. a) UV/Vis absorption spectra of RNase a1) and lysozyme a2) with complex 1

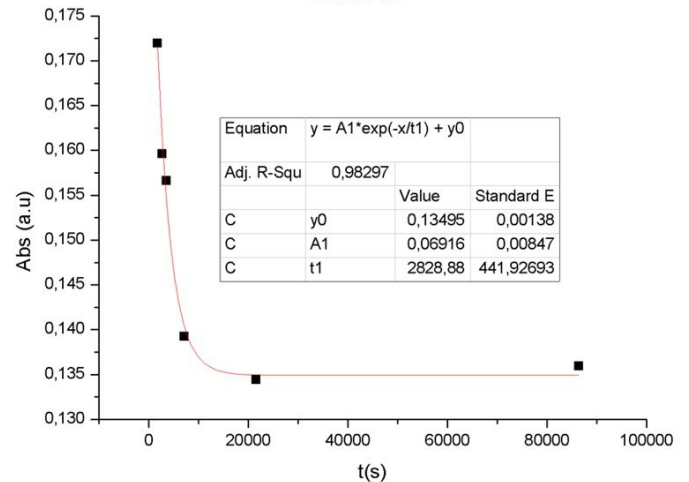
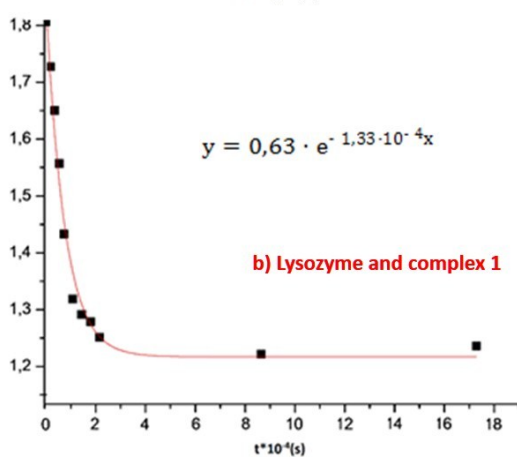
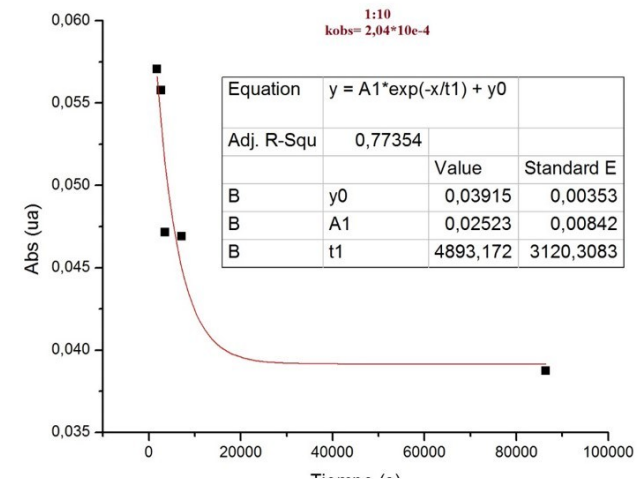
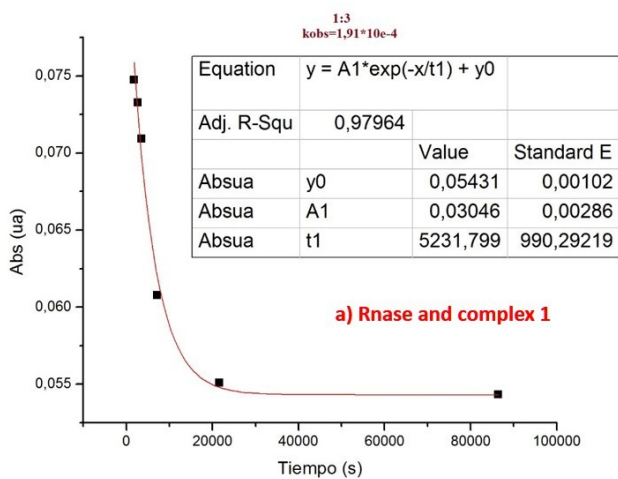


Figure SM7. Plots of the variation of the absorbance as a function of time of complex 1 with RNase a) and b) lysozyme.

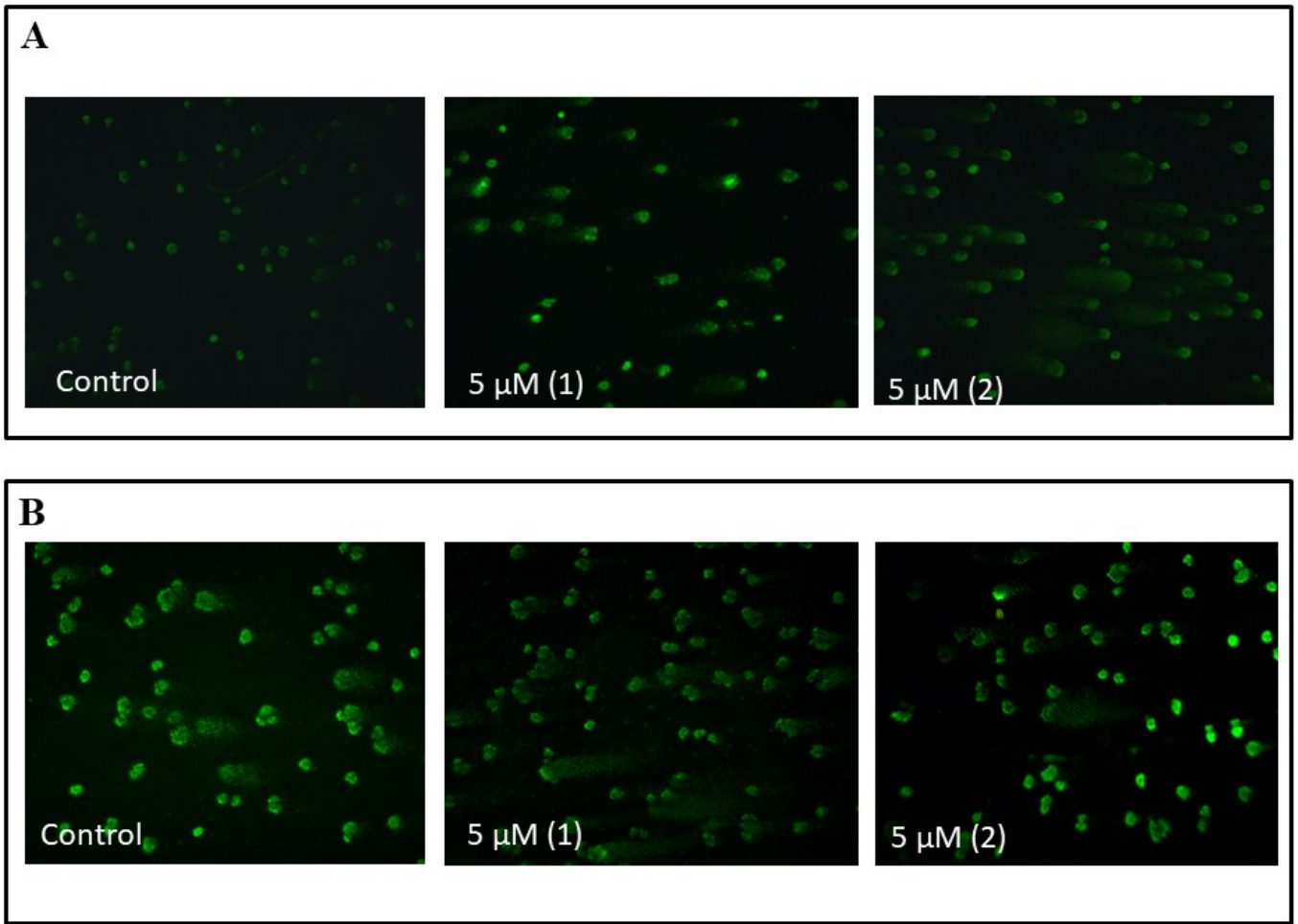


Figure SM8. Representative images of genotoxicity effects of complexes 1 and 2 on Jurkat (A) and L929 (B) cells.

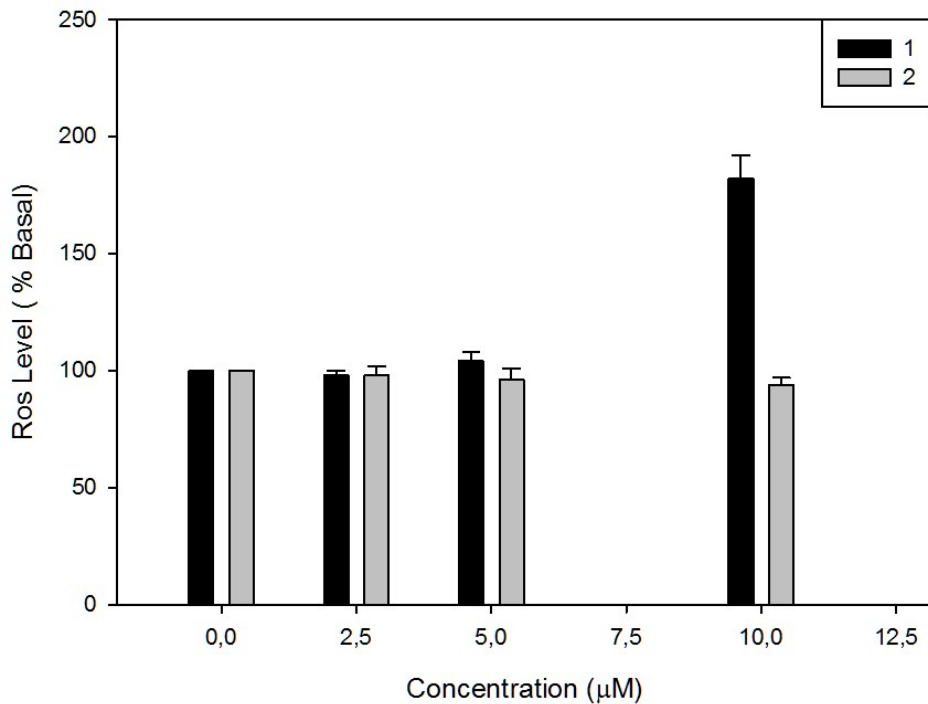


Figure SM9. Induction of ROS by compound 1 and 2 in Jurkat cell line. ROS production in the cells was evaluated through the oxidation of DHR-123 to rhodamine123. Results represent the mean \pm SEM, n = 12, *significant differences vs. control p < 0.01.

